ceramics

*Article*

# Multicriteria Assessment for Calculating the Optimal Content of Calcium-Rich Fly Ash in Metakaolin-Based Geopolymers

**Artem Sharko [1], Petr Louda [1], Van Vu Nguyen [1], Katarzyna Ewa Buczkowska [1,2], Dmitry Stepanchikov [3], Roberto Ercoli [4,*], Patrik Kascak [5] and Van Su Le [1,*]**

1 Department of Material Science, Faculty of Mechanical Engineering, Technical University of Liberec, Studentska 2, 461 17 Liberec, Czech Republic
2 Department of Materials Technology and Production Systems, Faculty of Mechanical Engineering, Lodz University of Technology, Stefanowskiego 1/15, 90-001 Lodz, Poland
3 Department of Energetics, Electrical Engineering, and Physics, Kherson National Technical University, 73008 Kherson, Ukraine
4 Department of Pure and Applied Sciences, University of Urbino, Via Ca' Le Suore 2/4, 61029 Urbino, Italy
5 Department of Industrial Engineering and Informatics, Faculty of Manufacturing, Technologies with the Seat in Prešov, The Technical University of Kosice, Bayerova 1, 08001 Presov, Slovakia
* Correspondence: roberto.ercoli@uniurb.it (R.E.); su.le.van@tul.cz (V.S.L.)

**Abstract:** This study examines the impact of calcium-rich fly ash as an additive on metakaolin-based geopolymers. Six types of fly ash (FA1-FA7) from different thermal power plants in the Czech Republic were collected and characterized based on their physical and chemical properties. The addition of fly ash into the geopolymers was evaluated through a multicriteria assessment that focused on density and mechanical properties. By using a multi-criteria approach, the assessment provides a comprehensive and holistic evaluation of the material, allowing for a more informed decision about the optimal addition of additives. This approach helps to minimize any negative impact on the material's properties while maximizing the utilization of the by-product. The result is an optimized geopolymer mixture with improved properties and increased sustainability, as the by-product is used beneficially. Furthermore, calcium content is the key factor that affects the physical properties of geopolymers by accelerating the curing time. This rapid process can result in reduced strength with increasing fly ash content. The multicriteria assessment revealed that the optimal condition is achieved using fly ash (FA2) from the Loucovice thermal power plant (5.2 wt.% Ca) that was treated at a temperature of 615 °C. The flexural strength of FA2-based geopolymers increased by 13% compared to concrete (standard). However, the addition of fly ash significantly reduced the compressive strength of geopolymers throughout the range of specimens. The Charpy impact strength of FA2 was higher than the standard due to the presence of unburned biomass solids in the ash structure that can absorb energy easily.

**Keywords:** geopolymers; fly ash; additives; mechanical properties



**Citation:** Sharko, A.; Louda, P.; Nguyen, V.V.; Buczkowska, K.E.; Stepanchikov, D.; Ercoli, R.; Kascak, P.; Le, V.S. Multicriteria Assessment for Calculating the Optimal Content of Calcium-Rich Fly Ash in Metakaolin-Based Geopolymers. *Ceramics* **2023**, *6*, 525–537. https://doi.org/10.3390/ceramics6010031

Academic Editors: Nichola Coleman and Andrew Paul Hurt

Received: 21 December 2022
Revised: 31 January 2023
Accepted: 10 February 2023
Published: 14 February 2023



## 1. Introduction

The environmental consequences that pollution and waste materials disposal created in the last decades brought the concept of new technologies and methods for processing large volumes of residual materials [1]. Portland cement is the main material employed in the construction industry. However, its manufacturing process emits a large amount of $CO_2$ [2]. The production of 1 ton of Portland cement requires 2.8 tons of raw materials and emits 0.8–1 ton of $CO_2$ into the atmosphere. Annually, cement plants emit up to 1.5 billion tons of $CO_2$. [3].

Geopolymers, high-strength products with properties similar to or superior to traditional ceramic and binder products, are used for the manufacture of prefabricated concrete structures and the immobilization of toxic waste [4–11]. Geopolymers have numerous benefits, including environmental safety and improved performance properties [12–18]. These materials do not ignite or produce smoke, have a high decomposition temperature, and are resistant to chemical attacks and water. They also have low thermal conductivity and high compressive strength, up to 100 MPa. The main constituents of geopolymers are raw materials and alkalis with natural aluminosilicate materials, such as kaolin, bentonite, montmorillonite, and calcined clay, being commonly used, as well as fly ash [19–23]. The materials are transformed into a dense 3D structure through alkaline activation [24].

Fly ash is a finely dispersed powder composed primarily of $SiO_2$, $Al_2O_3$, and $Fe_2O_3$, with a spherical shape. It is produced as a by-product of burning coal in power plants. However, the chemical composition and physical properties of fly ash vary due to differences in combustion conditions and biomass composition. The advantage of using fly ash in geopolymers is that the raw material has already been heat-treated, which saves significant amounts of energy. Fly ash is subjected to high incineration temperatures (1500–1800 °C), which causes the thermolysis and melting of inorganic minerals and results in solid waste dispersions. There are several potential benefits to using fly ash in geopolymers [25,26]. One advantage is that it can improve the material's mechanical properties, including strength and durability, resistance to cracking, shrinkage, weathering, and corrosion. The use of fly ash also has an environmental benefit by reducing the amount of material required in a geopolymer mix and reducing its carbon footprint.

Experimental studies were conducted on the strength, durability, and microstructure of geopolymers doped with different fly ashes. The impact of curing conditions and calcium content on the properties of metakaolin-based geopolymers with the addition of fly ash was thoroughly studied in the literature [27–34]. The formation of geopolymers is due to complex chemical and physical processes that impact their properties [35]. The reaction process can be accelerated by increasing the temperature [36,37], making curing conditions critical to the microstructure and final properties of the geopolymer [38]. A study [39] showed the effect of curing time on the high-temperature properties of a geopolymer mortar made with metakaolin and fly ash, with temperatures of 300, 600, and 900 °C, held for one hour. Results showed that after 25 days of atmospheric curing, the fly ash-based geopolymer had a compressive strength of 8.5 MPa, which is comparable to hot curing at 90 °C for four hours.

The use of calcium-rich fly ashes as binders and low-calcium fly ashes as fine-grained aggregates is one option for waste disposal and reducing gas emissions when synthesizing geopolymer materials [40]. This study examines several methods for producing fly ash-based mortars with a density of 2400 $kg/m^3$ and 80% total aggregate content. It is believed that the mechanical properties of geopolymers are related to their density, which is in turn related to the calcium content. Meanwhile, thermal properties are inversely proportional to density [41]. To synthesize low-density geopolymers, various blowing agents, such as surfactants in the form of liquid additives that trap air, are often used. The study aims to examine the physical properties of six different geopolymer compositions made from metakaolin, silica fume, recycled carbon fibers, and calcium-rich biomass fly ashes (FA1–7) from power plants in the Czech Republic.

## 2. Materials, Methods, Technology, and Equipment

### *2.1. Materials*

The inorganic two-component aluminosilicate binder (Table 1), (commercial name: Bausik LK), is manufactured by České lupkové závody, a.s. in the Czech Republic. It is based on metakaolin MK (Mephisto L05), ($\rho$ = 1220 $kg/m^3$; chemical composition: 40.10 wt.% $Al_2O_3$, 54.10 wt.% $SiO_2$, 0.80 wt.% $K_2O$, 1.10 wt.% $Fe_2O_3$, 1.80 wt.% $TiO_2$, 0.18 wt.% MgO, CaO 0.13 wt.%, 2.20 wt.% LOI; grain size: D50 = 3 μm, D90 = 10 μm), activated by an aqueous alkaline activator (A). The binder is known for its good adhesion, chemical resistance, and tolerance to temperature extremes. The mixing ratio is usually 5 parts metakaolin to 4 parts activator. Silica fume (SF) from Kema Morava—rehabilitation center a.s., Republic of Slovenia, ($\rho$ = 350 $kg/m^3$; chemical composition: 90 wt.% $SiO_2$, 1 wt.% $Al_2O_3$, 0.8 wt.% CaO, 1.5 wt.% MgO, 0.5 wt.% $Na_2O$; average grain size: 100 μm) was also added to the mortar.

**Table 1.** The chemical composition of raw materials.

| | $SiO_2$ (wt.%) | $Al_2O_3$ (wt.%) | $TiO_2$ (wt.%) | $Fe_2O_3$ (wt.%) | $K_2O$ (wt.%) | CaO (wt.%) | MgO (wt.%) | $Na_2O$ (wt.%) | C (wt.%) | LOI (wt.%) |
|---|---|---|---|---|---|---|---|---|---|---|
| MK | 54.10 | 40.10 | 1.80 | 1.10 | 0.80 | 0.13 | 0.18 | - | - | 2.20 |
| SF | 90 | 1 | - | - | - | 0.8 | 1.5 | 0.5 | - | - |
| CFs | - | - | - | - | - | - | - | - | >95 | - |

Recycled carbon fibers ($\rho$ = 1800 kg/$m^3$; chemical composition: >95 wt.% C; average length = 6 mm) were used as reinforcing fibers. The chunked fibers are well-suited for the production of dry and molding mortars.

Fly ashes (designated FA1–7, Figure 1) from thermal power plants in the Czech Republic were added to the geopolymer production. Their chemical compositions were determined using X-ray fluorescence (BRUKER S8 Tiger instrument, BRUKER, Karlsruhe, Germany) and a scanning electron microscope (SEM Carl Zeiss Ultra Plus, Oberkochen, Germany). Particle size and distribution were analyzed using a laser diffraction particle size analyzer (PSA model 1190 LD, AntonPaar, Frankfurt, Germany) following ISO Anton Paar, with results displayed in Tables 2–4.

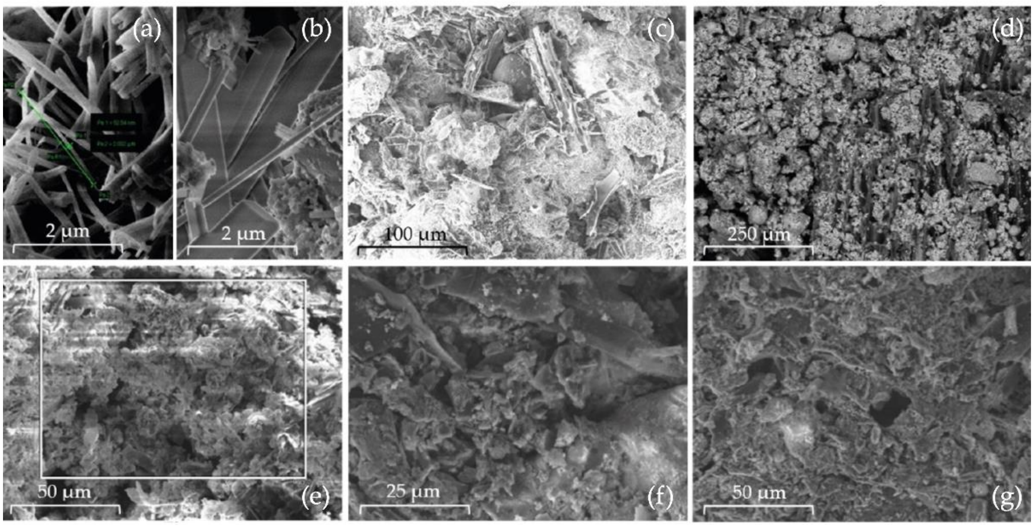


**Figure 1.** Microstructure of fly ash collected from various thermal power plants in the Czech Republic: (**a**) FA1—Louchovice CHP at 835 °C, (**b**) FA2—Louchovice CHP at 615 °C, (**c**) FA3—Cesky Krumlov, (**d**) FA4—Pisek, (**e**) FA5—Otin, (**f**) FA6—Mydlovy, (**g**) FA7—Trhove Sviny.

**Table 2.** The chemical composition of fly ash collected from the thermal power plants in the Czech Republic. FA1 and FA2 were collected from the same thermal plant at Louchovice but with different combustion temperatures (835 °C, and 615 °C). The rest of the ash FA3–7 was collected at 725 °C from various thermal plants.

| FLY ASH | FA1 | FA2 | FA3 | FA4 | FA5 | FA6 | FA7 |
|---|---|---|---|---|---|---|---|
| T (°C) | 835 | 615 | | | 725 | | |
| TPPs/Element (wt.%) | Louchovice | | Cesky Krumlov | Pisek | Otin | Mydlovy | Trhove Sviny |
| O | 40.4 | 43.2 | 32.3 | 32.7 | 39.5 | 60.3 | 33.1 |
| C | 32.9 | 30.0 | 50.0 | 50.7 | 32.5 | - | 43.2 |
| Ca | 9.4 | 5.2 | 9.8 | 3.3 | 10.7 | 9.4 | 5.4 |

**Table 2.** *Cont.*

| FLY ASH | FA1 | FA2 | FA3 | FA4 | FA5 | FA6 | FA7 |
|---|---|---|---|---|---|---|---|
| **T (°C)** | **835** | **615** | | | **725** | | |
| **TPPs/Element (wt.%)** | **Louchovice** | | **Cesky Krumlov** | **Pisek** | **Otin** | **Mydlovy** | **Trhove Sviny** |
| Si | 6.6 | 6.1 | 2.4 | 3.7 | 5.7 | 9.9 | 2.1 |
| K | 3.6 | 3.1 | 1.9 | 3.6 | 2.9 | 8.9 | 7.2 |
| Al | 1.9 | 3.5 | 0.9 | 1.1 | 1.5 | 1.2 | 0.9 |
| S | 1.4 | 1.3 | 0.9 | 1.2 | 1.0 | 2.8 | 3.2 |
| Mg | 1.0 | 2.3 | 0.5 | 0.9 | 2.1 | 1.5 | 1.3 |
| Cl | 0.8 | 0.5 | 0.5 | 1.0 | 0.5 | 2.3 | 1.4 |
| Na | - | - | 0.4 | 0.7 | 0.4 | 1.2 | 0.8 |
| Fe | 0.6 | 3.5 | 0.4 | 0.4 | 0.9 | 0.9 | 0.6 |
| P | - | - | 0.2 | 0.3 | 1.1 | 0.5 | 0.4 |
| Mn | - | - | - | 0.3 | 1.0 | 0.5 | 0.5 |
| Zn | - | - | - | 0.1 | 0.2 | 0.6 | - |
| Ti | - | - | - | 0.1 | - | - | - |

**Table 3.** Crystalline phases of FA1–7 were detected by XRD analysis.

| FLY ASH | Crystalline Phase—Chemical Formula (wt.%) | | | | | | |
|---|---|---|---|---|---|---|---|
| | **Calcite $CaCO_3$** | **Quartz $SiO_2$** | **Syngenite $K_2Ca(SO_4)_2 \cdot H_2O$** | **Magnesite $MgCO_3$** | **Aluminum Oxide $Al_2O_3$** | **Arcanite $K_2SO_4$** | **Corundum $Al_2O_3$** |
| FA1 | 35.2 | 37.1 | 27.7 | - | - | - | - |
| FA2 | 42.7 | 55.8 | - | 0.9 | 0.5 | - | - |
| FA3 | 35.2 | 37.1 | - | - | - | 27.7 | - |
| FA4 | 34.0 | 35.2 | - | - | - | 30.8 | - |
| FA5 | 39.7 | 39.0 | - | - | - | 21.3 | - |
| FA6 | 39.9 | 38.2 | - | - | - | 21.9 | - |
| FA7 | 31.3 | 29.7 | - | - | - | 38.4 | 0.6 |

**Table 4.** Laser beam particle size analysis of fly ashes (Volume, Number, Surface, Rosin-Rammler). and parameters (D10, D50, D90, Mean Size, Span, D [5,3]).

| FLY ASH | Grain Size Parameters | Volume | Number | Surface | Rosin-Rammler |
|---|---|---|---|---|---|
| FA1 | D10 (µm) | 20.851 | 16.626 | 18.645 | 20.049 |
| | D50 (µm) | 39.737 | 21.821 | 30.307 | 40.132 |
| | D90 (µm) | 63.698 | 38.889 | 56.161 | 62.539 |
| | Mean Size (µm) | 43.127 | 26.364 | 36.331 | 42.904 |
| | Span | 1.078 | 1.020 | 1.238 | 1.059 |
| | D [5,3] (µm) | 46.416 | - | - | - |
| FA2 | D10 (µm) | 18.015 | 1.4756 | 14.453 | 18.000 |
| | D50 (µm) | 39.510 | 1.7204 | 26.462 | 39.174 |
| | D90 (µm) | 65.290 | 14.378 | 55.507 | 64.571 |
| | Mean Size (µm) | 42.493 | 4.293 | 32.722 | 42.416 |
| | Span | 1.197 | 7.500 | 1.551 | 1.189 |
| | D [5,3] (µm) | 46.507 | - | - | - |
| FA3 | D10 (µm) | 20.459 | 15.848 | 18.017 | 19.972 |
| | D50 (µm) | 41.021 | 20.997 | 30.212 | 41.019 |
| | D90 (µm) | 66.306 | 38.346 | 57.873 | 65.314 |
| | Mean Size (µm) | 44.202 | 25.529 | 36.579 | 44.032 |
| | Span | 1.118 | 1.071 | 1.319 | 1.105 |
| | D [5,3] (µm) | 47.818 | - | - | - |

**Table 4.** *Cont.*

| FLY ASH | Grain Size Parameters | Volume | Number | Surface | Rosin-Rammler |
|---|---|---|---|---|---|
| FA4 | D10 (µm) | 22.000 | 16.851 | 19.259 | 21.899 |
| | D50 (µm) | 42.902 | 22.632 | 33.463 | 42.787 |
| | D90 (µm) | 66.899 | 42.355 | 59.257 | 66.134 |
| | Mean Size (µm) | 45.781 | 27.657 | 38.735 | 45.632 |
| | Span | 1.047 | 1.127 | 1.195 | 1.034 |
| | D [5,3] (µm) | 49.073 | - | - | - |
| FA5 | D10 (µm) | 16.279 | 0.01157 | 0.01798 | 13.019 |
| | D50 (µm) | 41.021 | 0.02069 | 0.3592 | 39.771 |
| | D90 (µm) | 70.329 | 0.03702 | 44.283 | 81.091 |
| | Mean Size (µm) | 43.960 | 0.04670 | 13.696 | 46.123 |
| | Span | 1.318 | 1.230 | 123.218 | 1.712 |
| | D [5,3] (µm) | 49.018 | - | - | - |
| FA6 | D10 (µm) | 15.723 | 0.4177 | 1.7900 | 14.723 |
| | D50 (µm) | 39.789 | 0.4968 | 19.464 | 38.732 |
| | D90 (µm) | 69.142 | 1.7044 | 53.559 | 71.771 |
| | Mean Size (µm) | 42.931 | 0.8589 | 25.218 | 43.420 |
| | Span | 1.343 | 2.590 | 2.660 | 1.473 |
| | D [5,3] (µm) | 47.966 | - | - | - |
| FA7 | D10 (µm) | 21.204 | 16.708 | 18.884 | 20.647 |
| | D50 (µm) | 39.611 | 22.247 | 31.144 | 40.043 |
| | D90 (µm) | 62.222 | 39.711 | 55.415 | 61.254 |
| | Mean Size (µm) | 42.807 | 26.821 | 36.514 | 42.616 |
| | Span | 1.036 | 1.034 | 1.173 | 1.014 |
| | D [5,3] (µm) | 45.820 | - | - | - |

### *2.2. Chemical Composition of the Geopolymers*

The weight ratio components of the geopolymer fly ash based referring to the metakaolin (MK) are given in Table 5.

**Table 5.** Physical characteristics and weight ratios (related to MK) of each geopolymer component.

| | Metakaolin (MK) | Activator (A) | Fly Ash (FA1–7) | Carbon Fibers (CFs) | Silica Fume (SF) |
|---|---|---|---|---|---|
| Density—$\rho$ (kg/m$^3$) | 1220 | 1640 | 625.89<br>645.53<br>669.08<br>667.89<br>702.92<br>692.05<br>623.23 | 1800 | 350 |
| Particle size (µm) | 20 | - | 15–10,000 | 6000 | 100 |
| Components ratios | 1 | 0.9 MK | 1 MK<br>0.75 MK<br>0.50 MK | 0.02 MK | 0.08 MK |

The metakaolin and the aqueous alkaline solution were mixed mechanically for 4 min until a homogeneous mortar was achieved. Fly ash was then added and stirred for 3 min, followed by the slow addition of carbon fibers to maintain fiber length and ensure even distribution. The mixture was poured into molds, covered with polyethylene film to prevent shrinkage, and cured for 28 days at room temperature, keeping the volume constant but changing the mass of the samples.

### *2.3. Testing Methods and Multicriteria Optimization*

In simple terms, the optimization of a geopolymer mixture aims to improve its physical properties, such as density and strength (flexural, compressive, and impact), by using a scalar function that gives a linear ranking of the results. This is achieved by reducing the density and converting vector estimates to scalar ones, as the target orientations and dimensions are different. The scalar function, represented by Equation (1), is based on the extreme values of the mixture.

$$F(y_i) = \sum_{j=1}^{n} \Delta y_{ij} \tag{1}$$

where $\Delta y_{ij}$ is the deviation (Equation (2)) from the intended target according to the *j*-th sign.

$$\Delta y_{ij} = \left| y_i - c_{j,extr} \right| \tag{2}$$

where

$c_{j,extr} = y_{j,max}$ is the maximization of the *j*-th analyzed characteristic of the feature space,

$c_{j,extr} = y_{j,min}$ is the minimization of the *j*-th analyzed characteristic of the feature space.

A common scale is required to measure all signs. Deviation of the *j*-th feature from the point $c_j$ ($c_j \pm \Delta y_j$) determines the distance from the target.

The matrix (Equation (3)) correlates the fly ash content in the composition of the geopolymer mixture at the experimental values of physical parameters as follows:

$$R = \begin{pmatrix} & \Pi_1 & \Pi_2 & \dots & \Pi_n \\ q_1 & \delta y_{11} & \delta y_{12} & \dots & \delta y_{1n} \\ q_2 & \delta y_{21} & \delta y_{22} & \dots & \delta y_{2n} \\ \dots & \dots & \dots & \dots & \dots \\ q_m & \delta y_{m1} & \delta y_{m2} & \dots & \delta y_{mn} \end{pmatrix} \tag{3}$$

where

$q_1 \dots q_m$ is fly ash content in the geopolymer mortar,

$\Pi_1 \dots \Pi_n$ is the physical parameters of the geopolymer,

*i* is line number,

*j* is column number.

The relative deviation (Equation (4)) of the *j*-th feature from the target is determined as follows:

$$\delta y_{ij} = \begin{cases} \frac{\left| y_{ij} - c_j \right|}{y_{j,\max -} c_j};\ y_{ij} > c_j \\ \frac{\left| y_{ij} - c_j \right|}{c_j - y_{j,min}};\ y_{ij} < c_j \end{cases} \tag{4}$$

In simple terms, the optimization process uses $c_j$, as a parameter, which is the maximum value of the physical parameters being processed. Equation (4) transforms these dimensional values into relative values within a scale of 0.1. However, this can lead to the loss of certain features or zeroing them out if the elements in the matrix (Equation (3)) match the value of "$c_j$", which corresponds to $\delta y_{ij} = 0$. When using additive convolution, this leads to the loss of the corresponding feature from the overall assessment of the object, and when using multiplicative convolution, to zeroing it. An obvious way to avoid such situations is to expand the upper (for maximum) or lower (for minimum) limit of each feature $c_j$ in the same percentage. To avoid this, the maximum or minimum limit for each feature "$c_j$" can be increased or decreased by 1%.

The matrix "*R*" takes into account both maximizing and minimizing elements in consideration. It is important to consider multiple criteria, not just one, to find the optimal composition with the best properties and lowest density. Different multicriteria utility functions were used in the theoretical analysis [42].

*Additive convolution:*

$$y_a = \delta y_i = \sum_{j=1}^{n} \omega_j\, \delta y_{ij}', \tag{5}$$

where $\omega_j$ is the weight coefficient of the *j*-th feature, $\sum\limits_{j=1}^{n} \omega_j = 1$

*Power multiplicative convolution:*

$$y_a = \delta y_i = \sum_{j=1}^{n} \omega_j \, \delta y_{ij}{}' \tag{6}$$

*Additional multiplicative convolution:*

$$y_{md} = \delta y_i = 1 - \prod_{j=1}^{n} \left(1 - \omega_j \, \delta y_{ij}\right) \tag{7}$$

The best composition of fly ash is considered to have a minimum functional value (Equations (5)–(7)).

*Wald criterion (minimum-maximum):*

$$Z_v = \min_i \max_j \delta y_{ij} \tag{8}$$

*Laplace criterion (minimum-minimum):*

$$Z_L = \min_i \min_j \delta y_{ij}{}', \tag{9}$$

*Hurwitz criterion:*

$$Z_{hw} = \min_i \left\{ \rho \min_j \delta y_{ij} + (1-\rho) \max_j \delta y_{ij} \right\} \tag{10}$$

where $0 \leq \rho \leq 1$—the indicator of pessimism was considered equal to 0.5 in the calculations.

The flexural and compressive tests were performed on an Instron (Model 4202) Universal Testing Machine with a load cell of 10 kN, and a crosshead speed of 2.5 mm/min at room temperature. They were estimated using the standard UNI EN 1015-11:2019 [43]. Three samples of the same specimens with dimensions of $(30 \times 30 \times 150)$ mm$^3$ were tested for flexural strength with a loading span of 100 mm. The compressive strength was determined on the $(30 \times 30 \times 30)$ mm$^3$ residual pieces of the flexural tests.

The Charpy impact strength was carried out using a PIT-C Series Pendulum Impact Testing Machine on samples of $(20 \times 19 \times 60)$ mm$^3$, following the standard ISO 148-1:2016 test method [44].

## 3. Results

The most useful physical property of the materials to explain the mass-volume dependency is density. Figure 2 displays the densities of seven calcium-rich fly ash geopolymers with the ash content of maximum values of 1, 0.75, and 0.5 (e.g., GP.FA1-1 max; ... ; GP.FA7-0.5 max), as per Table 6.

Considering the geopolymer standard, the change in density when fly ash is added to the mortar is largely determined by the particle size distribution. Chemical reactions between the binder and additives during geopolymerization also play a key role in affecting the resulting density. Determining the contribution of each of these components to the overall density is a critical technological task that affects the production of geopolymers. The practical benefit of this understanding provides quantifiable recommendations on where to obtain fly ash of the required density, which is highly valuable in optimizing geopolymer production.

Mechanical tests were performed, which are crucial for characterizing new materials that will be subjected to loads. The results regarding strength were compared to two standards: (i) geopolymer without fly ash (STD-1) and (ii) concrete, i.e., Baumit 25 (STD-2).

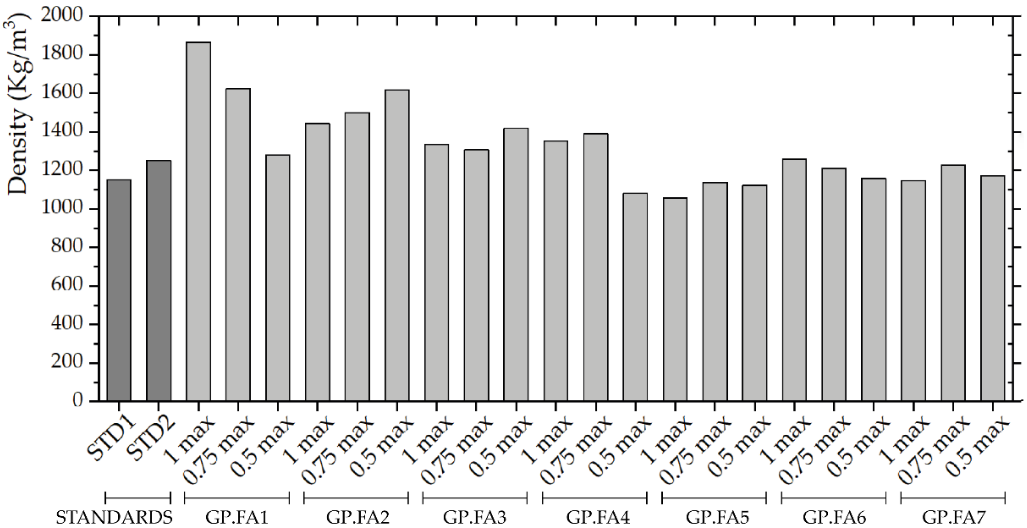


**Figure 2.** The densities of geopolymers strictly depend on the type of fly ash added: Loucovice at 615 °C (1), and 835 °C (2), Cesky Krumlov (3), Pisek (4), Otin (5), Mydlovy (6), and Trchov Svin (7). STD1 and STD2 are the standards: geopolymer without fly ash, and concrete Baumit 25.

**Table 6.** Physical parameters for the optimization of fly ash-based geopolymer compositions.

| Geopolymer—GP | Fly Ash—FA Content | Density—$\rho$ (kg/m$^3$) | Flexural Strength—$\sigma_f$ (MPa) | Compressive Strength—$\sigma_c$ (MPa) | Charpy Impact Strength—$\sigma_i$ (KJ/m$^2$) |
|---|---|---|---|---|---|
| GP.FA1 | 1 max | 1850 | $7.14 \pm 0.31$ | $34.33 \pm 3.53$ | $12.22 \pm 0.34$ |
| | 0.75 max | 1610 | $6.34 \pm 0.45$ | $32.27 \pm 2.57$ | $8.26 \pm 0.30$ |
| | 0.5 max | 1250 | $5.55 \pm 0.05$ | $27.96 \pm 4.05$ | $8.35 \pm 0.32$ |
| GP.FA2 | 1 max | 1430 | $5.50 \pm 0.17$ | $27.88 \pm 2.55$ | $8.25 \pm 0.70$ |
| | 0.75 max | 1510 | $5.37 \pm 0.05$ | $27.18 \pm 1.04$ | $13.57 \pm 0.55$ |
| | 0.5 max | 1620 | $5.48 \pm 0.08$ | $29.44 \pm 1.51$ | $27.17 \pm 0.33$ |
| GP.FA3 | 1 max | 1300 | $4.44 \pm 0.12$ | $16.77 \pm 0.67$ | $8.46 \pm 1.14$ |
| | 0.75 max | 1290 | $4.88 \pm 0.07$ | $19.66 \pm 0.82$ | $14.30 \pm 0.51$ |
| | 0.5 max | 1400 | $4.27 \pm 0.11$ | $24.18 \pm 2.08$ | $8.26 \pm 0.39$ |
| GP.FA4 | 1 max | 1330 | $4.06 \pm 0.05$ | $15.42 \pm 2.10$ | $4.54 \pm 0.38$ |
| | 0.75 max | 1400 | $4.54 \pm 0.05$ | $20.03 \pm 1.45$ | $4.57 \pm 0.33$ |
| | 0.5 max | 1120 | $4.46 \pm 0.14$ | $21.97 \pm 2.70$ | $3.55 \pm 0.24$ |
| GP.FA5 | 1 max | 1070 | $3.35 \pm 0.01$ | $11.13 \pm 1.12$ | $3.60 \pm 0.29$ |
| | 0.75 max | 1120 | $3.79 \pm 0.12$ | $16.06 \pm 1.09$ | $5.53 \pm 0.38$ |
| | 0.5 max | 1050 | $4.28 \pm 0.08$ | $20.51 \pm 0.87$ | $4.24 \pm 0.25$ |
| GP.FA6 | 1 max | 1240 | $3.71 \pm 0.05$ | $21.17 \pm 1.26$ | $4.06 \pm 0.23$ |
| | 0.75 max | 1190 | $4.29 \pm 0.03$ | $20.79 \pm 2.88$ | $9.07 \pm 0.35$ |
| | 0.5 max | 1140 | $4.67 \pm 0.17$ | $31.43 \pm 1.78$ | $6.34 \pm 0.36$ |
| GP.FA7 | 1 max | 1160 | $3.36 \pm 0.05$ | $14.38 \pm 0.39$ | $6.27 \pm 0.23$ |
| | 0.75 max | 1220 | $3.50 \pm 0.01$ | $15.57 \pm 0.41$ | $5.63 \pm 0.18$ |
| | 0.5 max | 1140 | $4.18 \pm 0.21$ | $21.76 \pm 0.46$ | $3.48 \pm 0.37$ |

Figure 3 displays the results of flexural tests for different proportions (1–0.75–0.5 MK) of calcium-rich fly ash added to the mortar.

This is an experimental and quantitative confirmation of the influence of the chemical composition and microstructure of fly ash on the physical and mechanical properties of geopolymers. The use of calcium-rich ash hastens the setting time but reduces the strength of the geopolymer. As observed, with an increase in fly ash dispersion above 450 m$^2$/kg, the water requirement of the dissolved mixture increases and the flexural strength decreases.

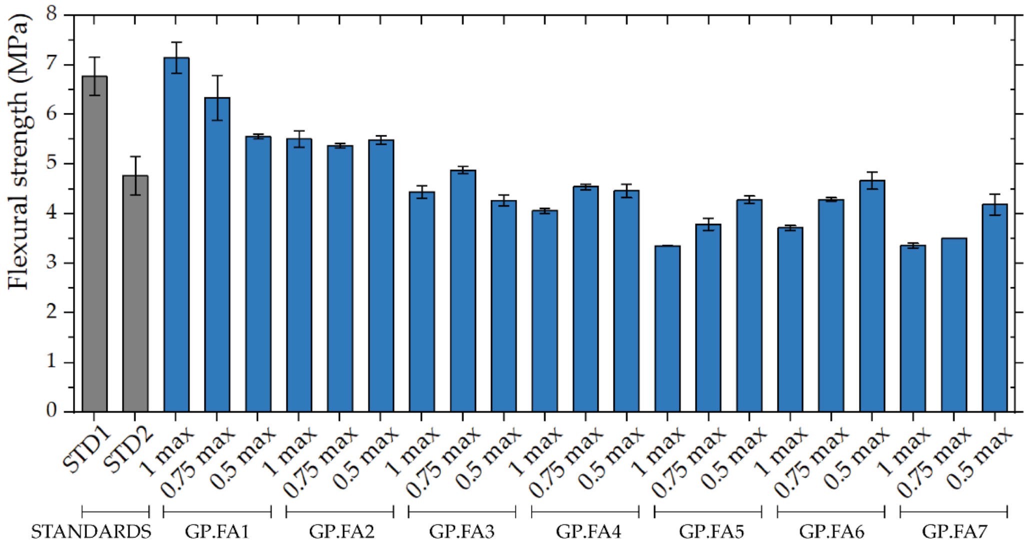


**Figure 3.** The flexural strength of the geopolymers synthesized with fly ash from thermal power plants was evaluated. The standards used were STD1, which is a geopolymer without fly ash, and STD2, which is the concrete Baumit 25.

Figure 4 displays the results of mechanical compression tests conducted for various fly ash proportions.

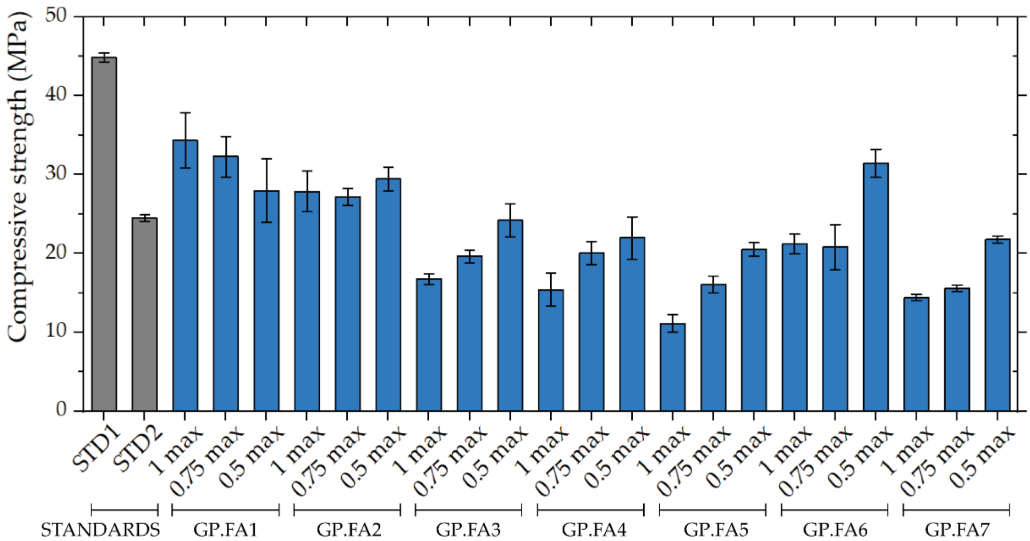


**Figure 4.** Compressive strengths of geopolymers with FA1–7.

Additionally, Charpy impact strengths (Figure 5) were obtained for the various geopolymers synthesized with the previously mentioned fly ash amounts.

The results ambiguously demonstrate the effect of fly ash addition on impact strength concerning the amount added, which could be due to the ash structure. Although geopolymer molecules may have similar chemical compositions, their different particle sizes can lead to polydispersity, causing variations in the physical properties of the material. The changes in mechanical properties of geopolymers doped with the various fly ash types are observed on their surfaces, as depicted in Figure 6.

The images in Figure 6 depict carbon fibers that are evenly distributed, intending to enhance the material mechanical properties and counteract the potential impact of micro-cracks. The images also show unburned parts of the biomass, which could weaken the mechanical properties of the geopolymer paste by adding ash.

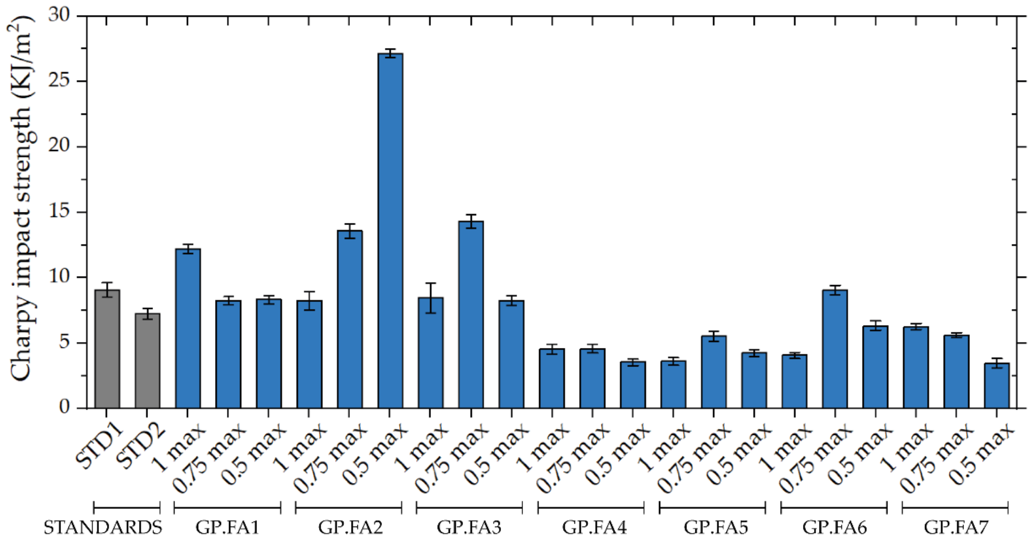


**Figure 5.** Charpy impact strength of geopolymers with FA1–7.

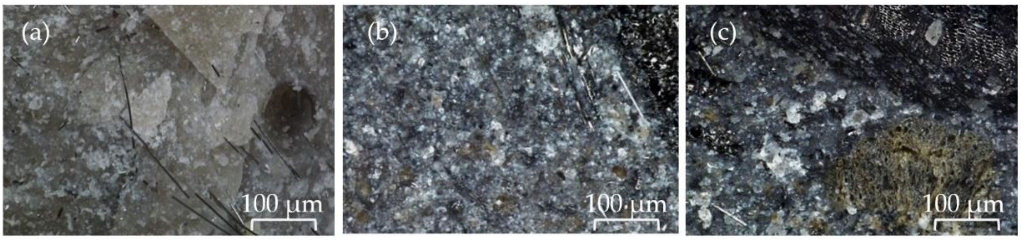


**Figure 6.** SEM images of geopolymer with an FA4 content of 0, 0.5, and 0.75 max, marked as (**a**), (**b**), and (**c**), respectively.

A multi-criteria assessment based on fuzzy logic algorithms determines the fly ash content in the geopolymer mixture, which affects its strength. The physical and mechanical measurements (Table 6) are presented as a collection of individual measurements and should be condensed into a single indicator represented by the arithmetic average for calculation purposes and to optimize the fly ash content and distribution within the structure of geopolymers.

The matrix of dimensionless geopolymer parameters calculated by the formula (Equation (4)), as well as the values of convolutions (Equations (5)–(7)) and criteria (Equations (8)–(10)), are shown in Table 7. The calculations were performed under the assumption that all criteria are equally important. The coincidence and degree of adequacy of each generalizing function must be considered. The analysis of the results reveals that the additive convolution, additional multiplicative convolution, Laplace, and Hurwitz criteria indicate FA2 as the most optimal, which is in agreement with the result obtained by the Wald criterion. Hence, the best geopolymer composition is with the addition of FA2 at a content of 0.5–0.75 maximum.

**Table 7.** Matrix of dimensionless values of parameters of geopolymers, as well as values of convolutions and criteria.

| GP | $\rho$ | $\sigma_f$ | $\sigma_c$ | $\sigma_i$ | min | max | $\frac{\min + \max}{2}$ | $y_a$ | $y_{ms}$ | $y_{md}$ |
|---|---|---|---|---|---|---|---|---|---|---|
| GP.FA1 | 1.000 | 0.018 | 0.014 | 0.635 | 0.014 | 1.000 | 0.507 | 0.417 | 0.114 | 0.374 |
| | 0.703 | 0.226 | 0.101 | 0.800 | 0.101 | 0.800 | 0.451 | 0.458 | 0.337 | 0.394 |
| | 0.259 | 0.429 | 0.285 | 0.796 | 0.259 | 0.796 | 0.528 | 0.442 | 0.398 | 0.379 |
| GP.FA2 | 0.481 | 0.442 | 0.288 | 0.800 | 0.288 | 0.800 | 0.544 | 0.503 | 0.471 | 0.419 |
| | 0.580 | 0.477 | 0.318 | 0.578 | 0.318 | 0.580 | 0.449 | 0.488 | 0.475 | 0.407 |
| | 0.716 | 0.448 | 0.222 | 0.011 | 0.011 | 0.716 | 0.363 | 0.349 | 0.168 | 0.313 |

**Table 7.** *Cont.*

| GP | $\rho$ | $\sigma_f$ | $\sigma_c$ | $\sigma_i$ | min | max | $\frac{\min + \max}{2}$ | $y_a$ | $y_{ms}$ | $y_{md}$ |
|---|---|---|---|---|---|---|---|---|---|---|
| GP.FA3 | 0.321 | 0.718 | 0.760 | 0.792 | 0.321 | 0.792 | 0.556 | 0.648 | 0.610 | 0.510 |
| | 0.309 | 0.605 | 0.637 | 0.548 | 0.309 | 0.637 | 0.473 | 0.525 | 0.505 | 0.432 |
| | 0.444 | 0.763 | 0.445 | 0.800 | 0.444 | 0.800 | 0.622 | 0.613 | 0.590 | 0.488 |
| GP.FA4 | 0.358 | 0.817 | 0.817 | 0.955 | 0.358 | 0.955 | 0.657 | 0.737 | 0.691 | 0.561 |
| | 0.444 | 0.692 | 0.622 | 0.954 | 0.444 | 0.954 | 0.699 | 0.678 | 0.654 | 0.527 |
| | 0.099 | 0.713 | 0.539 | 0.997 | 0.099 | 0.997 | 0.548 | 0.587 | 0.441 | 0.479 |
| GP.FA5 | 0.037 | 1.000 | 1.000 | 0.994 | 0.037 | 1.000 | 0.518 | 0.758 | 0.439 | 0.581 |
| | 0.099 | 0.887 | 0.790 | 0.914 | 0.099 | 0.914 | 0.507 | 0.672 | 0.502 | 0.530 |
| | 0.012 | 0.759 | 0.601 | 0.968 | 0.012 | 0.968 | 0.490 | 0.585 | 0.275 | 0.480 |
| GP.FA6 | 0.247 | 0.906 | 0.573 | 0.975 | 0.247 | 0.975 | 0.611 | 0.675 | 0.595 | 0.530 |
| | 0.185 | 0.757 | 0.589 | 0.766 | 0.185 | 0.766 | 0.476 | 0.574 | 0.502 | 0.467 |
| | 0.124 | 0.659 | 0.137 | 0.880 | 0.124 | 0.880 | 0.502 | 0.450 | 0.315 | 0.390 |
| GP.FA7 | 0.148 | 0.998 | 0.862 | 0.883 | 0.148 | 0.998 | 0.573 | 0.723 | 0.579 | 0.558 |
| | 0.222 | 0.961 | 0.811 | 0.910 | 0.222 | 0.961 | 0.592 | 0.726 | 0.630 | 0.558 |
| | 0.124 | 0.784 | 0.548 | 1.000 | 0.124 | 1.000 | 0.562 | 0.614 | 0.480 | 0.495 |
| | | | | | *LaPlace* | *Vlad* | *Hurwitz* | | | |
| | | | | | 0.011 | 0.580 | 0.363 | | | |

## 4. Conclusions

The study investigates the multicriteria optimization of the geopolymer mixture, considering physical properties, such as density and mechanical strengths (flexural, compressive, and Charpy impact), to optimize geopolymer characteristics by minimizing density. In particular, the research explains the effect of calcium-rich fly ashes (FA1–7) from power plants in the Czech Republic on the physical properties and microstructures of geopolymers.

The advantage of the current method, which moves from vector estimates to scalar ones, over existing methods is that it addresses the issues of formula optimization and mathematical superiority evaluation. This method considers different target orientations and dimensions, providing a more accurate evaluation of the properties of the geopolymer mixture. Scalar estimates allow for a more accurate calculation of the properties of the mixture, providing a representation of the material performance. This increased accuracy makes the method a more reliable tool for optimizing the formula of the geopolymer mixture. The use of scalar estimates also provides a clear and concise comparison of the properties of the mixture. This makes it easier to determine the best formula, as the results are presented clearly and straightforwardly. Overall, the advantage of this method is that it provides a more accurate and reliable evaluation of the properties of the geopolymer mixture, making it a valuable tool for optimizing the formula and improving the material performance. These properties are crucial for determining the suitability of the geopolymer for various applications. Moreover, the geopolymer is comparable to other materials, such as conventional building materials and other polymers.

The multi-criteria assessment found that FA2 from the Loucovice thermal power plant (combustion temperature = 615 °C) offers the highest mechanical properties of GP. The flexural strength decreased by 30% with ash containing 10.7 wt.% Ca (FA5), but increased by 13% with ash containing 5.2 wt.% Ca (FA2) compared to the standards. The compressive strengths are significantly reduced but can be improved by adding up to 50% of the maximum amount of ash. It is known that the use of calcium-rich ash significantly decreases the setting time and strength of geopolymers, as shown by microstructural studies, which produced stable and homogeneous geopolymers with densely packed matrixes, affecting strength.

**Author Contributions:** Conceptualization, P.L. and A.S.; methodology, P.L., D.S. and V.S.L.; data curation, P.L. and K.E.B.; validation, P.L., K.E.B., V.V.N., D.S. and R.E.; formal analysis, A.S., V.S.L., R.E., P.K. and V.V.N.; investigation, A.S. and V.V.N. All authors have read and agreed to the published version of the manuscript.

**Funding:** This research was funded by the Institutional Endowment for the Long-Term Conceptual Development of Research Institutes (numbers fund: IP–117), as provided by the Ministry of Education, Youth, and Sports of the Czech Republic in the year 2022.

**Institutional Review Board Statement:** Not applicable.

**Informed Consent Statement:** Not applicable.

**Data Availability Statement:** The data presented in this study are available on request from the corresponding author.

**Acknowledgments:** The results of the project “Development of geopolymer composites as a material for the protection of hazardous wrecks and other critical underwater structures against corrosion” registration number TH8002007 were obtained through the financial support Technology Agency of the Czech Republic within the Epsilon Program, in the Call 2021 M-ERA.Net2. This publication was written at the Technical University of Liberec with the support of the Institutional Endowment for the Long-Term Conceptual Development of Research Institutes, as provided by the Ministry of Education, Youth, and Sports of the Czech Republic in the year 2022.

**Conflicts of Interest:** The authors declare no conflict of interest.

## References

1. Khale, D.; Chaudhary, R. Mechanism of geopolymerization and factors influencing its development: A review. *J. Mater. Sci.* **2007**, *42*, 729–746. [CrossRef]
2. Naghizadeh, A.; Ekolu, S.O. Effect of Mix Parameters on Strength of Geopolymer Mortars-Experimental Study. In Proceedings of the Sixth International Conference on Durability of Concrete Structures at Leeds, West Yorkshire, UK, 18–20 July 2018.
3. Hattaf, R.; Aboulayt, A.; Samdi, A.; Lahlou, N.; Touhami, M.O.; Gomina, M.; Moussa, R. Reusing Geopolymer Waste from Matrices Based on Metakaolin or Fly Ash for the Manufacture of New Binder Geopolymeric Matrices. *Sustainability* **2021**, *13*, 8070. [CrossRef]
4. Merabtene, M.; Kacimi, L.; Clastres, P. Elaboration of geopolymer binders from poor kaolin and dam sludge waste. *Heliyon* **2019**, *5*, e01938. [CrossRef]
5. Kheradmand, M.; Abdollahnejad, Z.; Pacheco-Torgal, F. Drying shrinkage of fly ash geopolymeric mortars reinforced with polymer hybrid fibers. *Proc. Inst. Civ. Eng. Constr. Mater.* **2020**, *173*, 28–40. [CrossRef]
6. Friedlander, L.R.; Weisbrod, N.; Garb, Y.J. Climatic and soil-mineralogical controls on the mobility of trace metal contamination released by informal electronic waste (e-waste) processing. *Chemosphere* **2019**, *232*, 130–139. [CrossRef]
7. Zhang, Z.; Zhu, Y.; Yang, T.; Li, L.; Zhu, H.; Wang, H. Conversion of local industrial wastes into greener cement through geopolymer technology: A case study of high-magnesium nickel slag. *J. Clean. Prod.* **2017**, *141*, 463–471. [CrossRef]
8. Aboshia, A.M.A.; Rahmat, R.A.; Zain, M.F.M.; Ismail, A. Enhancing mortar strengths by ternary geopolymer binder of metakaolin, slag, and palm ash. *Int. J. Build. Pathol. Adapt.* **2017**, *35*, 438–455. [CrossRef]
9. Shaikh, F.U.A. Mechanical and durability properties of fly ash geopolymer concrete containing recycled coarse aggregates. *Int. J. Sustain. Built Environ.* **2016**, *5*, 277–287. [CrossRef]
10. De Oliveira, L.B.; de Azevedo, A.R.; Marvila, M.T.; Pereira, E.C.; Fediuk, R.; Vieira, C.M.F. Durability of geopolymers with industrial waste. *Case Stud. Constr. Mater.* **2022**, *16*, e00839. [CrossRef]
11. Cilla, M.S.; Colombo, P.; Morelli, M.R. Geopolymer foams by gel casting. *Ceram. Int.* **2014**, *40*, 5723–5730. [CrossRef]
12. Rovnaník, P. Effect of curing temperature on the development of hard structure of metakaolin-based geopolymer. *Constr. Build. Mater.* **2010**, *24*, 1176–1183. [CrossRef]
13. Le, V.S.; Louda, P. Research of Curing Time and Temperature-Dependent Strengths and Fire Resistance of Geopolymer Foam Coated on an Aluminum Plate. *Coatings* **2021**, *11*, 87. [CrossRef]
14. Nguyen, V.V.; Le, V.S.; Louda, P.; Szczypiński, M.M.; Ercoli, R.; Růžek, V.; Łoś, P.; Prałat, K.; Plaskota, P.; Pacyniak, T.; et al. Low-Density Geopolymer Composites for the Construction Industry. *Polymers* **2022**, *14*, 304. [CrossRef]
15. Le Chi, H.; Louda, P.; Le Van, S.; Volesky, L.; Kovacic, V.; Bakalova, T. Composite Performance Evaluation of Basalt Textile-Reinforced Geopolymer Mortar. *Fibers* **2019**, *7*, 63. [CrossRef]
16. Szczypinski, M.M.; Louda, P.; Exnar, P.; Le Chi, H.; Kovačič, V.; Van Su, L.; Voleský, L.; Bayhan, E.; Bakalova, T. Evaluation of Mechanical Properties of Composite Geopolymer Blocks Reinforced with Basalt Fibres. *Manuf. Technol.* **2018**, *18*, 861–865. [CrossRef]
17. Ercoli, R.; Laskowska, D.; Nguyen, V.V.; Le, V.S.; Louda, P.; Łoś, P.; Ciemnicka, J.; Prałat, K.; Renzulli, A.; Paris, E.; et al. Mechanical and Thermal Properties of Geopolymer Foams (GFs) Doped with By-Products of the Secondary Aluminum Industry. *Polymers* **2022**, *14*, 703. [CrossRef]
18. Mostefa, F.; Bouhamou, N.-E.; Aggoune, S.; Mesbah, H. Elaboration of geopolymer cement based on dredged sediment. *J. Mater. Eng. Struct.* **2019**, *6*, 39–51.

19. Kan, L.; Wang, W.; Wang, J.; Duan, X. Preparation and Tensile Property of Metakaolin-Fly Ash Based Engineered Geopolymer Composites. *Jianzhu Cailiao Xuebao J. Build. Mater.* **2019**, *22*, 5. [CrossRef]
20. Mas, M.A.; Tashima, M.M.; Payá, J.; Borrachero, M.; Soriano, L.; Monzó, J. A Binder from Alkali Activation of FCC Waste: Use in Roof Tiles Fabrication. *Key Eng. Mater.* **2016**, *668*, 411–418. [CrossRef]
21. Ojha, P.N.; Materials, I.N.C.F.C.A.B.; Singh, B.; Kaura, P.; Singh, A. Lightweight geopolymer fly ash sand: An alternative to fine aggregate for concrete production. *Res. Eng. Struct. Mater.* **2021**, *7*, 3. [CrossRef]
22. Sivasakthi, M.; Jeyalakshmi, R. Effect of change in the silica modulus of sodium silicate solution on the microstructure of fly ash geopolymers. *J. Build. Eng.* **2021**, *44*, 102939. [CrossRef]
23. Muduli, S.D.; Nayak, B.D.; Mishra, B.K. Geopolymer fly ash building brick by atmospheric curing. *Int. J. Chem. Sci.* **2014**, *12*, 1086–1094.
24. Sun, H.; Zeng, L.; Peng, T. Research Status and Progress of High-value Utilization of Coal Fly Ash. *Cailiao Daobao Mater. Rep.* **2021**, *35*, 03010–03015. [CrossRef]
25. Li, C.; Li, J.; Ren, Q.; Zhao, Y.; Jiang, Z. Degradation mechanism of blended cement pastes in sulfate-bearing environments under applied electric fields: Sulfate attack vs. decalcification. *Compos. Part B Eng.* **2022**, *246*, 110255. [CrossRef]
26. Li, J.; Zhang, W.; Li, C.; Monteiro, P.J. Eco-friendly mortar with high-volume diatomite and fly ash: Performance and life-cycle assessment with regional variability. *J. Clean. Prod.* **2020**, *261*, 121224. [CrossRef]
27. Koumoto, T. Production of High Compressive Strength Geopolymers Considering Fly Ash or Slag Chemical Composition. *J. Mater. Civ. Eng.* **2019**, *31*, 8. [CrossRef]
28. Sanjay, K.; Rakesh, K. Tailoring Geopolymer Properties through Mechanical Activation of Fly Ash. 2010. Available online: https://www.semanticscholar.org/paper/Tailoring-geopolymer-properties-through-mechanical-Kumar-Kumar/85937be89e1451b54467c2095ad2fda2bc73abc5 (accessed on 7 October 2022).
29. Saif, M.S.; El-Hariri, M.O.; Sarie-Eldin, A.I.; Tayeh, B.A.; Farag, M.F. Impact of Ca+ content and curing condition on durability performance of metakaolin-based geopolymer mortars. *Case Stud. Constr. Mater.* **2022**, *16*, e00922. [CrossRef]
30. Guo, X.; Pan, X. Effects of Steel Slag on Mechanical Properties and Mechanism of Fly Ash–Based Geopolymer. *J. Mater. Civ. Eng.* **2020**, *32*, 2. [CrossRef]
31. Dinesh, H.T.; Shivakumar, M.; Dharmaprakash, M.S.; Ranganath, R.V. Influence of reactive $SiO_2$ and $Al_2O_3$ on mechanical and durability properties of geopolymers. *Asian J. Civ. Eng.* **2019**, *20*, 1203–1215. [CrossRef]
32. Buchwald, A.; Dombrowski, K.; Weil, M. The influence of calcium content on the performance of geopolymeric binder especially the resistance against acids. *Proc. World Geopolym.* **2005**, *29*, 6.
33. Yaswanth, K.; Revathy, J.; Gajalakshmi, P. Strength, durability and micro-structural assessment of slag-agro blended based alkali activated engineered geopolymer composites. *Case Stud. Constr. Mater.* **2022**, *16*, e00920. [CrossRef]
34. Radhi, M.S.; Al-Ghaban, A.M.H.; Al-Hydary, I.A.D. RSM Optimizing the Characteristics of Metakaolin based Geopolymer Foam. *J. Phys. Conf. Ser.* **2021**, *1973*, 012151. [CrossRef]
35. Caicedo, M.A.V.; De Gutiérrez, R.M. Synthesis of ternary geopolymers based on metakaolin, boiler slag and rice husk ash. *DYNA* **2015**, *82*, 104–110. [CrossRef]
36. Elimbi, A.; Tchakoute, H.; Kondoh, M.; Manga, J.D. Thermal behavior and characteristics of fired geopolymers produced from local Cameroonian metakaolin. *Ceram. Int.* **2014**, *40*, 4515–4520. [CrossRef]
37. Talakokula, V.; Singh, R.; Karunakaran, V. Effect of delay time and duration of steam curing on compressive strength and microstructure of fly ash based geopolymer concrete. *Indian Concr. J.* **2015**, *89*, 69–72.
38. Yin, X.; Wang, X.; Fang, Y.; Ding, Z. Influence of curing age on high-temperature properties of additive manufactured geopolymer mortar. *E3S Web Conf.* **2020**, *218*, 03019. [CrossRef]
39. Kamal, M.A. Recycling of Fly Ash as an Energy Efficient Building Material: A Sustainable Approach. *Key Eng. Mater.* **2016**, *692*, 54–65. [CrossRef]
40. Mahdi, S.N.; Hossiney, N.; Abdullah, M.M.A.B. Strength and durability properties of geopolymer paver blocks made with fly ash and brick kiln rice husk ash. *Case Stud. Constr. Mater.* **2022**, *16*, e00800. [CrossRef]
41. Kalinkin, A.M.; Gurevich, B.I.; Kalinkina, E.V.; Semushin, V.V. Synthesis of geopolymers based on mechanically activated low-calcium iron-rich fly ash. *Environ. Prog. Sustain. Energy* **2022**, *41*, e13733. [CrossRef]
42. Buketov, A.; Academy, U.K.S.M.; Sharko, A.; Zinchenko, D.; Stepanchikov, D. To the problem of ingredients optimization of composite materials based on epoxy resin. *Bull. Karaganda Univ.* **2017**, *86*, 37–44. [CrossRef]
43. Standards. Available online: https://standards.iteh.ai/catalog/standards/cen/14596d4c-119b-4a78-94e1-3fe481a29bde/en-1015-11-2019 (accessed on 7 October 2022).
44. ISO. Available online: https://www.iso.org/standard/63802.html (accessed on 7 October 2022).